

## A Variety of Activation Methods Employed in "Activated-Ion" Electron Capture Dissociation Mass Spectrometry: A Test against *Bovine* Ubiquitin 7+ Ions

HanBin Oh\* and Fred W. McLafferty†

Department of Chemistry and Interdisciplinary Program of Biotechnology, Sogang University, Seoul 121-742, Korea

\*E-mail: hanbinoh@sogang.ac.kr

†Department of Chemistry and Chemical Biology, Cornell University, Ithaca, NY 14853-1301, USA

Received November 27, 2005

Fragmentation efficiencies of various 'activated-ion' electron capture dissociation (AI-ECD) methods are compared for a model system of bovine ubiquitin 7+ cations. In AI-ECD studies, sufficient internal energy was given to protein cations prior to ECD application using IR laser radiation, collisions, blackbody radiation, or in-beam collisions, in turn. The added energy was utilized in increasing the population of the precursor ions with less intra-molecular noncovalent bonds or enhancing thermal fluctuations of the protein cations. Removal of noncovalent bonds resulted in extended structures, which are ECD friendly. Under their best conditions, a variety of activation methods showed a similar effectiveness in ECD fragmentation. In terms of the number of fragmented inter-residue bonds, IR laser/blackbody infrared radiation and 'in-beam' activation were almost equally efficient with ~70% sequence coverage, while collisions were less productive. In particular, 'in-beam' activation showed an excellent effectiveness in characterizing a pre-fractionated single kind of protein species. However, its inherent procedure did not allow for isolation of the protein cations of interest.

**Key Words :** Electron capture dissociation (ECD), Fourier-transform mass spectrometry (FTMS), Ubiquitin, Activated-ion ECD, In-beam ECD

### Introduction

When combined with various activation methods, electron capture dissociation (ECD) can provide extensive primary structure information even on large protein cations.<sup>1,7</sup> In contrast to classical tandem mass spectrometry (MS/MS) methods based on energetic activation, ECD backbone fragmentations occur in a random fashion, and thus give more detailed information. Extraordinary cleavage ability of ECD has enabled detailed characterizations of intact protein cations and localization of posttranslational modifications (PTMs), which has made possible a so-called "top-down" mass spectrometry approach.<sup>8-13</sup>

Additionally, ECD has a unique feature of conserving labile bonds during fragmentation of strong protein backbone manifolds.<sup>2,5,7</sup> This characteristic is manifested in some examples, which include its inertness to PTM groups that are weakly bonded and the conservation of weak noncovalent interactions, both inter-molecular and intra-molecular. While the former (PTM analysis), in most cases, plays a positive role in view of sequence coverage, the latter can be problematic since this often prohibits the separation of the two ECD fragments through remaining noncovalent interactions between them. Thus extensive efforts have been made to develop a method that can eliminate noncovalent interactions prior to ECD applications.<sup>3-5</sup>

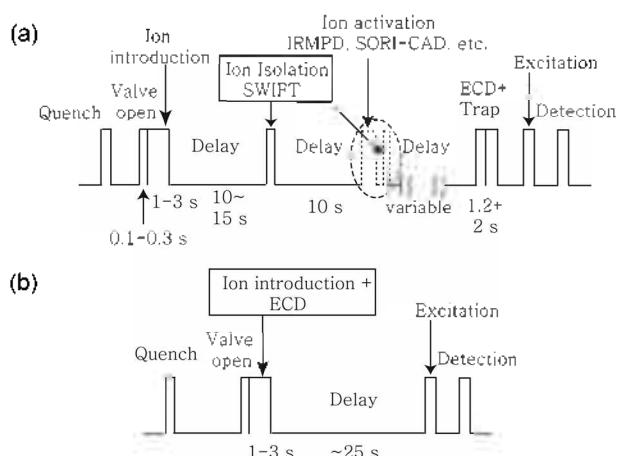
In general, a variety of energetic activation methods have been known to increase the precursor-ion populations with less noncovalent bonds or to give greater structural fluctuations that are favorable to ECD analysis.<sup>3,5,13-15</sup> Prominent examples include thermal heating, IR multiphoton absorp-

tion, and collisional activation, to name. Indeed, these methods have been shown to lead to more apparent fragments when applied together with ECD; so-called 'activated-ion ECD (AI-ECD)',<sup>15,16</sup> In more recent years, a few modified collision activation methods have also been demonstrated to exhibit unprecedented ECD fragmentation efficiencies; for example, 'in-beam' or 'plasma' ECD.<sup>3-5</sup>

With all these interesting advantages, there has been no systematic evaluation or comparison made about the relative efficiency of these activation methods in combination with ECD. Thus, we have here examined their relative efficiencies by comparing the fragmentation patterns for bovine ubiquitin 7+ cations that consist of 76 amino acids (8.6 kDa). Previously, it was reported that regular ECD of ubiquitin 7+ cations led to a relatively small number of fragments, most of which were from either N- or C-terminal region.<sup>15,16</sup> However, when IR multiphoton activation was given prior to an ECD procedure, extended fragmentations were observed to arise all across the primary sequence. In the present study, we will describe a variety of activation methods employed here and the associated fragmentation patterns for ubiquitin 7+ cations, in great detail.

### Experimental Section

A detailed description of the experimental setup can also be found elsewhere.<sup>1,5</sup> Experiments were performed on a 6-T Fourier-transform ion cyclotron resonance mass spectrometer (FTICR MS) with an ECD capability. *Bovine* ubiquitin was purchased from Sigma (St. Louis, MO, USA) and was used without further purification. Samples were



**Scheme 1.** Time-course of ICR events for (a) normal ECD and AI-ECD experiments, and (b) 'in-beam' ECD experiment. The activation event is represented in a dashed circle.

dissolved in a 92 : 6 : 2 (v/v/v) water:methanol:acetic acid solution with 20  $\mu\text{M}$  concentration. Electrospray was performed using a homebuilt nano-electrospray source. A potential of +1.2 kV was applied to a Pt wire inserted into a home-pulled capillary, a borosilicate tube (i.d. = 0.86 mm and o.d. = 1.5 mm). A commercial puller (PM 70, Sutter Instrument, Novato, CA, USA) was utilized in preparing for an electrospray emitter. Sprayed ions were transported through three stage quadrupole ion-guides into an ICR-cell and trapped by  $\text{N}_2$  gas collisional damping and electric pulsed-gating.

The time course of subsequent ICR events is represented in Scheme 1. In regular ECD with no activation step, a delay time of 10–15 s was given to the trapped cations before either activation or ECD procedure in order to achieve kinetic cool-down. Then, ubiquitin 7+ cations were isolated using a single stored waveform inverse Fourier transform (SWIFT) application and thereafter another 10 s delay was provided for further kinetic relaxation.<sup>17</sup> ECD application was carried out by exposing the isolated ubiquitin 7+ cations to 1.2 s electron beam pulse emitted from a Rh ribbon. The ribbon was positioned off-axis outside a superconducting magnet in order to allow for passage of  $\text{CO}_2$  IR laser radiation. Electrons were introduced into the ICR cell by pulse-gating on a stainless mesh plate, and its static current was maintained at 0.1–0.3  $\mu\text{A}$ . The electron kinetic energy was set to 0.5 eV. In the 'ECD' event of Scheme 1a, –1 V and –1 V potentials were given on the trapping plates of 'Spare 1' and 'Spare 2', respectively. Here, 'Spare 1' refers to the trapping plate closer to a Rh ribbon and 'Spare 2' to the ion introduction source. In the subsequent 'Trap' event, electrons were trapped in the ICR cell by changing potentials on both trapping plates to –1 V for reaction with protein ions to proceed. In 'in-beam' ECD experiments, 'ion-introduction' and 'electron-introduction' (ECD) were employed simultaneously (see Scheme 1b). In this procedure, the potentials on Spare 1 and 2 were adjusted to 6 and 5 V, respectively, which are the potentials normally used in the routine 'ion-introduction' event.

In the 'activated-ion' ECD (AI-ECD) experiments, except for 'in-beam' ECD, almost identical event sequences were employed.<sup>3</sup> To be more specific, two activation-related events were added to the regular ECD sequence; these events are marked in a dashed circle (see Scheme 1a). The second event in a dashed circle, *i.e.*, 'ion-isolation', was needed in order to eliminate fragment ions that could be generated during the activation procedure. For activation of protein cations, collisional activation,  $\text{CO}_2$  IR laser irradiation, thermal heating, and 'in-beam' ECD were utilized in turn. In the collision-assisted AI-ECD, the degree of collisional activation was controlled by alternatively tuning two experimental parameters such as excitation attenuation in dB in the manufacturer's software (Odyssey 3.0, Extrel, Madison, WI, USA) and the length of sustained-off resonance irradiation collisional activation (SORI-CAD) procedure.<sup>18–20</sup> As a collision gas, a high-purity nitrogen gas was used. Likewise, for  $\text{CO}_2$  IR laser (25W, Synrad, Mulilteo, WA, USA) radiation activation, a wide range of intensity and length of  $\text{CO}_2$  IR laser beam were also tested to optimize the overall performance. In the case of thermal heating activation, blackbody infrared radiation from the vacuum chamber was utilized by raising the temperature of the chamber from 25 to 175  $^\circ\text{C}$ . For this purpose, temperature was controlled using a heat blanket around the chamber that is equipped with feedback adjustments. In 'in-beam' ECD experiments, as shown in Scheme 1b, three events of ion introduction, activation, and electron introduction (ECD) were executed simultaneously. In this experiment, activation was achieved *via* collisions between incoming molecular ions and collision gas molecules. Activated molecular ions were then involved in electron capture, further leading to ECD fragmentation. In this 'in-beam' experiment, a careful caution was taken in preparing for electrospray solution so that ubiquitin 7+ cations, which were chosen as a model system, were most abundant in the precursor molecular ion population. For each spectrum, at least 20 time-domain data were co-added.

## Results and Discussion

**Regular ECD for Bovine Ubiquitin 7+ Cations, ( $M + 7H$ )<sup>7+</sup>.** Figure 1(a) and (b) represent a precursor-ion mass spectrum and a regular ECD product ion spectrum, respectively, obtained for ubiquitin 7+ cations, ( $M + 7H$ )<sup>7+</sup>, with no pre-activation step. The latter, as expected, exhibits a relatively simple spectrum with a small number of fragment ions (Figure 1(b)). This spectrum shows two abundant peaks at  $m/z$  1,428 and 1,716 as well as many low abundance peaks at  $< 1,700$   $m/z$ . These two highly abundant peaks arose from electron capture by 7+ precursor cations, and are composed of two complementary ECD fragments held together by complex noncovalent bonds.<sup>2,15,16</sup> They represent so-called 'reduced ions'; the former at  $m/z$  1,448 is 6+• singly reduced ions, ( $M + 7H$ )<sup>6+•</sup>, and the latter is 5+•• doubly reduced ions, ( $M + 7H$ )<sup>5+••</sup>. Extra hydrogen atom(s) in the reduced ions allows us to experimentally distinguish the reduced ions from

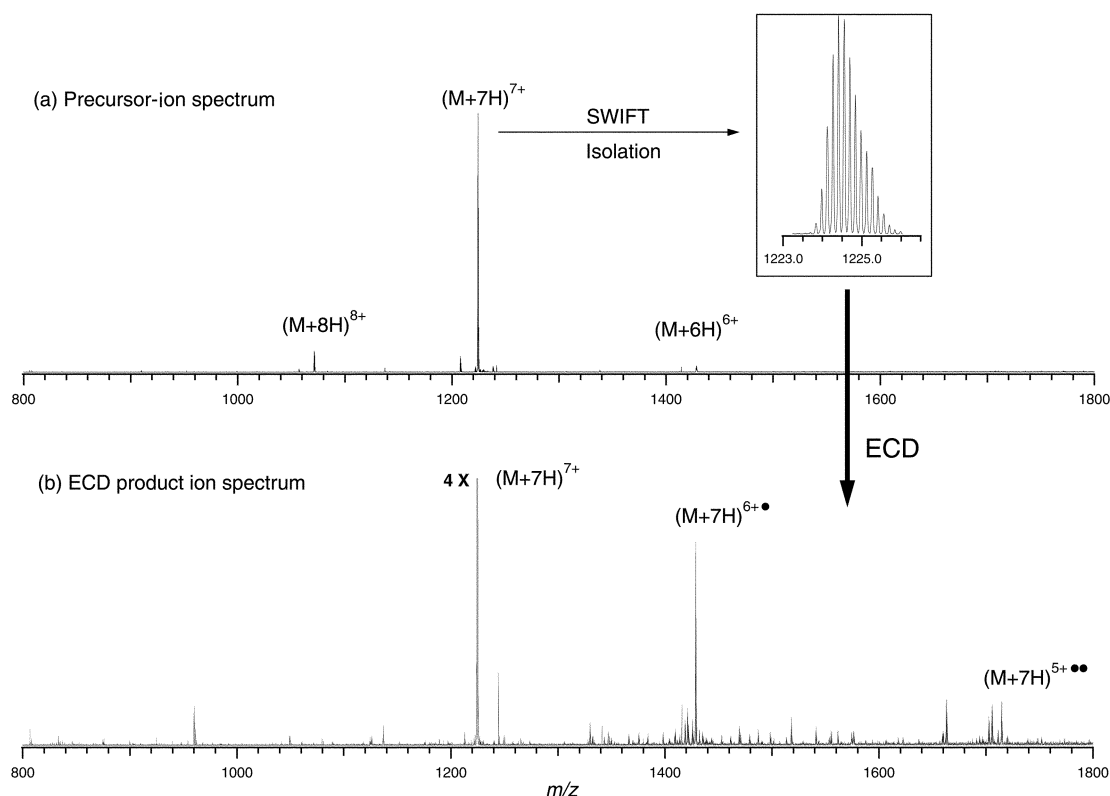


**Figure 1.** (a) A precursor-ion mass spectrum produced by electrospraying a 20  $\mu\text{M}$  ubiquitin 92 : 6 : 2 (v : v : v) water : methanol : acetic-acid solution. Inset: ubiquitin 7+ cations isolated by a single SWIFT waveform. (b) ECD product ion mass spectrum of the isolated ubiquitin 7+ cations obtained using a regular ECD method with no activation procedure.

the normal molecular ions of  $(M + 6H)^{6+}$  and  $(M + 5H)^{5+}$ .

Identities of ECD fragments in Figure 1(b) were denoted in the analysis histogram of Figure 2(a). The analysis was made with an aid of THRASH retrieving algorithm.<sup>21</sup> Most products were assigned as  $c$  or  $b$  ions, consistent with previous reports.<sup>1-5,15,16</sup> The ECD fragment pattern in Figure 2(a) shows that ECD fragments appear mostly in N- or C-terminus, while in the central sequence region, fewer fragments were observed. This result is consistent with partially-unfolded conformations of ubiquitin 7+ cations suggested in ion-mobility studies.<sup>22-25</sup> Noncovalent bonds such as salt-bridge, hydrogen bonding, and van der Waals forces are responsible for such folded conformations.

To improve ECD sequence coverage, it is necessary to remove as much noncovalent bonds as possible. In general, a practical choice is to increase Coulombic repulsions within a protein cation by attaching more protons, and this approach has been shown to successfully induce more extensive fragmentations throughout an entire backbone chain.<sup>2</sup> Another approach for eliminating noncovalent bonds is to add sufficient internal energy to protein cations.<sup>15,16</sup> As discussed earlier, various activation methods such as collisions, IR laser radiation, or blackbody radiation can heat up molecules to remove the existing intra-molecular non-covalent bonds. In the present study, experimental focus is made on the latter approach in order to seek the optimal activation method for providing the best sequence

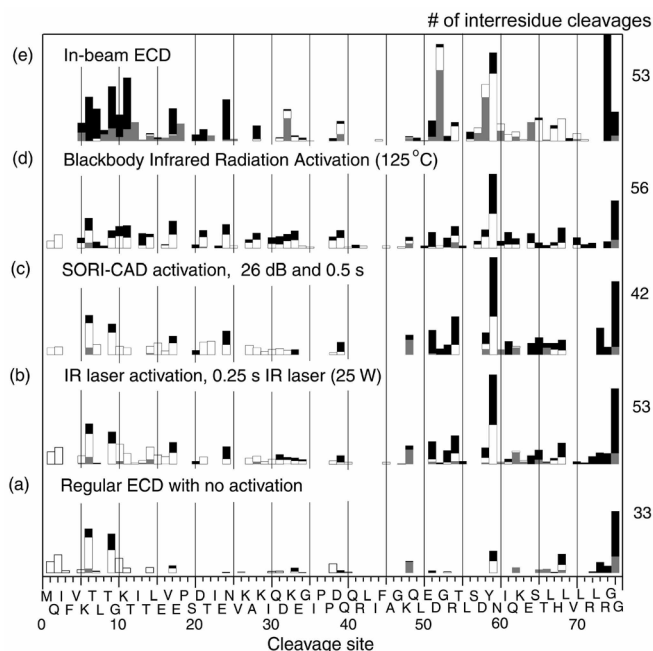


**Figure 2.** Normalized abundances (vertical bars) of various AI-ECD dissociation products denoted along cleavage sites (sequence). Black segment (top of vertical bar),  $c$  ions; open segment,  $b$  ions; gray segment,  $b + b \cdot y$  ions. (a) regular ECD, (b) IR laser activation, (c) SORI-CAD activation, (d) blackbody infrared radiation activation, and (e) 'in-beam' activation. The numbers of cleaved interresidue bonds are denoted in the right column.

information when combined with ECD.

**Activation by IR Laser Absorption.** As previously reported, CO<sub>2</sub> IR laser radiation (10.6  $\mu\text{m}$ ) can thermally activate ubiquitin 7<sup>-</sup> cations and thus subsequent ECD application for activated species led to much enhanced fragmentations throughout the entire backbone.<sup>15,16</sup>

In the present study, 25-W IR laser beam was continuously irradiated for 0.25 s prior to ECD application. This relatively short laser turn-on time was chosen so that activation by IR radiation was just sufficient enough to open up folded conformations without inducing significant backbone dissociations. After IR laser beam, ubiquitin 7<sup>+</sup> cations at  $m/z$  1,224 were re-isolated using a single SWIFT waveform for further ECD analysis. This procedure inevitably introduced a short time interval between IR laser irradiation and ECD application; 0.07 s was the shortest time interval needed for a broadband SWIFT application. Fragmented ions brought about by IR laser irradiation were, if any, isolated out in the ICR cell by this procedure. Subsequent ECD application was executed immediately after SWIFT isolation. The resulting fragmentation spectrum and its analysis are shown in Figure 2b and 3, respectively.

The number of fragmented ions considerably increased when compared to that of the regular ECD spectrum; 53 versus 33. The abundances of 6 $\bullet$  or 5 $\bullet\bullet$  reduced ions, which are not useful in providing protein sequence information, are observed to dramatically decrease, while the relative abundances of fragmented ions increase in return. The increased abundance of individual fragments has led to higher signal-to-noise ratio and thus helped us easily identify

ECD products in the complicated mass spectra. To be specific, a number of new peaks arose in the sequence regions 15-34 and 50-67 which did not appear in the previous regular ECD experiments. This clearly shows that removal of noncovalent bonds in these regions was achieved by 0.25 s CO<sub>2</sub> IR irradiation. This means that 0.25 s CO<sub>2</sub> IR radiation provided ubiquitin 7<sup>+</sup> cations with the energy sufficient enough to overcome the unfolding enthalpy,  $\Delta H_{\text{unfolding}}$ , whose value was previously determined to be  $32 \pm 2$  kJ/mol in the temperature range up to 100  $^{\circ}\text{C}$ .<sup>16</sup>

In separate experiments, the effect of IR laser power on the activation efficiency was also investigated by adjusting the laser power to 25, 50, or 100% of 25-W full power. But in these experiments, the laser was turned on for 1.2 s *during*, not *before*, ECD execution in order to minimize protein conformational cooling that might occur during the intervening SWIFT procedure. The resulting fragmentation spectra obtained with 25, 50, and 100% laser power are represented in Figure 4(a), (b), and (c), respectively. The comparison shows that the increased laser power wouldn't much affect the total amount of sequence information; 54, 56, and 52 out of 75 inter-residue bonds, respectively. At high laser power, several *b* type ions also appeared, particularly, at amino sequences 32, 52, and 58. However, the amount of *de novo* sequence information did not increase significantly from 52 of the aforementioned IR laser AI-ECD experiment (Figure 2b). It is because the sequence information provided by IRMPD (*b* or *y* ions) overlaps substantially with that (*c* or  $\bullet$  ions) of AI-ECD. Furthermore, IRMPD at high powers was found to even interfere

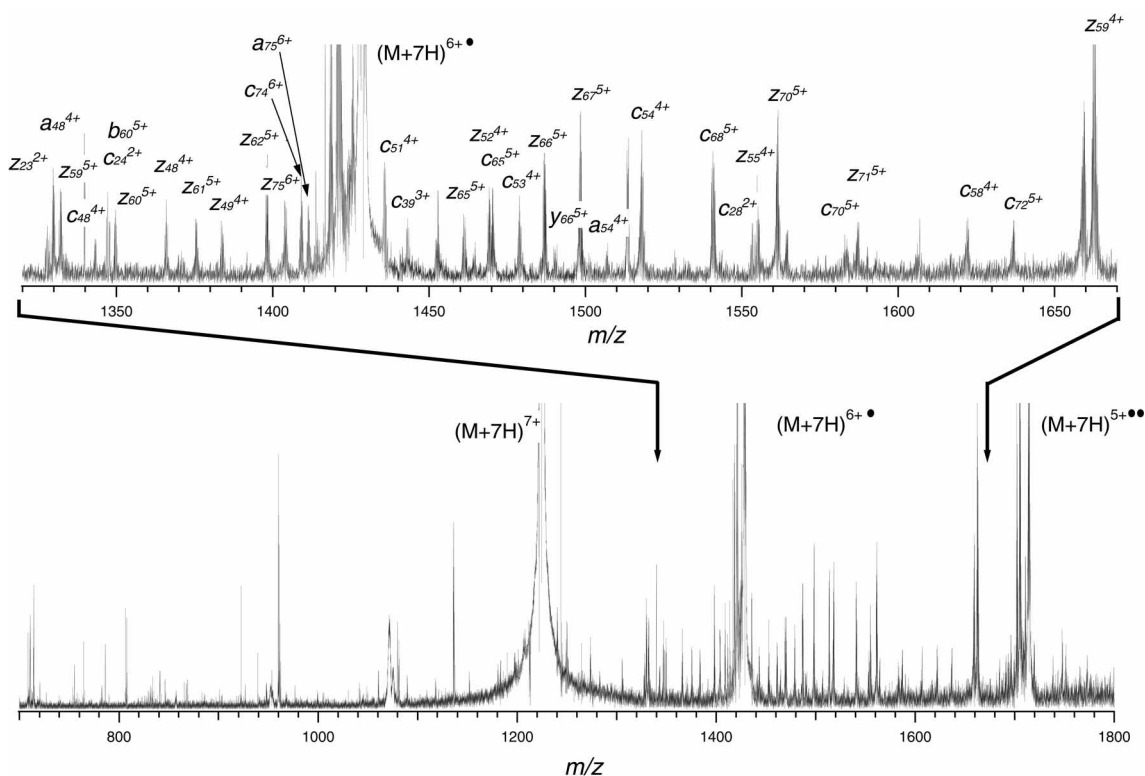


**Figure 3.** (a) AI-ECD product-ion mass spectrum obtained using a 0.25s radiation of 25 W CO<sub>2</sub> laser. (b) Zoomed-out spectrum in the range of  $m/z$  1,350 to 1,450.

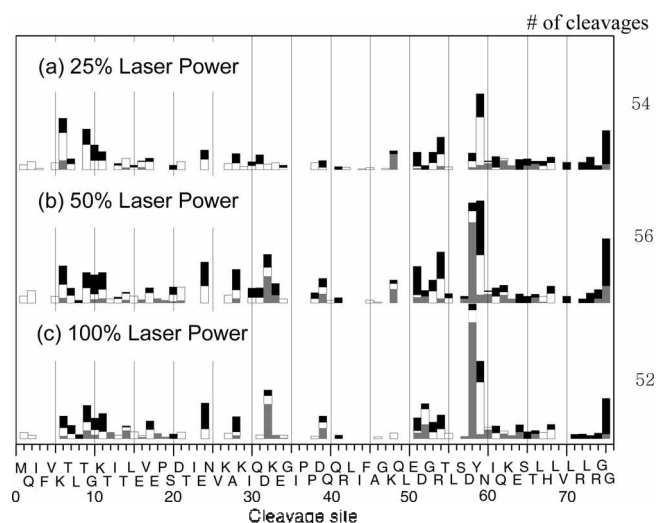


**Figure 4.** Normalized abundances obtained by simultaneous application of both ECD and (a) 100% IR laser power (25 W), (b) 50% IR laser power, and (c) 25% IR laser power.

with ECD by causing secondary dissociations; THRASH algorithm counts only the primary products that have N- or C- terminus and thus the secondary products can not be identified.<sup>21</sup>

**Collisional Activation by SORI-CAD.** Collisionally-activated dissociation (CAD), the mostly used dissociation method in mass spectrometry, can also be utilized as an activation tool in AI-ECD.<sup>26</sup> In this experiment, SORI-CAD (Sustained Off-Resonance Irradiation-Collisionally Activated Dissociation) was employed that is an FTMS version of CAD utilizing a slightly off-resonanced RF field to add collisional energy to molecular ions.<sup>18</sup> Experimental event-sequence was very similar to that of IR-laser AI-ECD, except that SORI-CAD was utilized instead of IR laser radiation (see Figure 1(a)). In this experiment,  $-1.4$  kHz off-resonance RF field was applied.

As shown in Figure 2(c), SORI-CAD AI-ECD produced many fragment ions, but the extent of sequence information was smaller than the IR laser activated method did; 42 amino acid sequence information only. Among many experimental parameters, the intensity and the length of SORI-CAD were found to be important. Tuning over a wide range of SORI-CAD intensity showed that 26.0 dB scale in the manufacturer's control software produced the most fragmentations. Higher attenuation values, *i.e.*, lower SORI-CAD intensity, failed to sufficiently activate molecular ions, while the lower attenuation induced too much CAD fragmentations. The optimal activation was achieved in a relatively narrow tuning range, *i.e.*,  $\sim 2$  dB. In the case of the length of SORI-CAD application, it was varied from 0.1 to 3 s at an appropriate interval. Activation efficiency increased proportionally up to 0.6 s, but the length longer than 0.6 s was found to provide gradually deteriorated activation, finally showing no activation with  $> 2.0$  s length. This is largely due to the fact that high collision gas pressure, which is necessary for SORI-CAD to operate, could not be sustained long time in the cell because of collision-gas diffusion

and pumping-out. Furthermore, as the length of SORI-CAD application gradually increased, unfolded conformers presumably started to fold back to original conformations in which extensive intra-molecular noncovalent bonds exist. According to previous reports, ubiquitin 7<sup>+</sup> ions fold back within 1-2 s.

In view of implementation, SORI-CAD AI-ECD was not easy to use since fine tuning of its intensity and length was required for successful use. Furthermore, introduction of a collision gas into the ICR cell provided the pumping system a heavy load which requires rather long pumping-out delay time. More importantly, a narrow range of optimal conditions made it difficult to achieve the 'best' sequencing results.

**Activation by Blackbody Infrared Radiation.** ECD was performed at elevated temperatures in order to increase the population of the precursor-ions that have less noncovalent bonds.<sup>15,16</sup> The best performance was made at 125 °C with its result being represented in Figure 2(d). The total number of backbone cleavages and the fragmentation pattern are comparable to those of other AI-ECD methods. This strongly indicates that the added energies resulted in removal of noncovalent bonds in a specific way rather than in a random fashion, though given by different methods. At higher or lower temperatures, activation occurred relatively inefficiently. At higher temperatures, more noncovalent bonds would be removed. Thus, the conformers with extended linear structures that are more amenable to ECD analysis are considerably populated. However, too high temperatures are not necessarily advantageous since it would interfere with ECD performance by leading to secondary dissociations. In this study, the balance is made at 125 °C. The optimal temperature can vary depending on various factors such as the chemical composition and global potential-energy-landscape of the molecular ions that governs its secondary and tertiary structures.

On the other hand, it should be emphasized that from a practical point of view, running ECD experiments at high temperatures is not highly recommendable since it usually takes several hours to raise and to later lower back the temperature of the ICR cell for normal analyses of other samples. This practical, *but not intrinsic*, drawback might be critical to analytical laboratories in which a main function is mandated for analysis of diverse chemical/biological samples.

**In-beam Activation.** The procedure employed in an 'in-beam' ECD experiment is different from that of other AI-ECD experiments (see Figure 1b).<sup>3-5</sup> Whereas in other activation methods protein cations were pre-stored in the ICR cell before being exposed to various activations, in this procedure protein ions and electrons were introduced simultaneously into the cell along with a collision gas N<sub>2</sub>. A multitude of collisions occurred among these species with relatively high kinetic energies, and thus induced substantial collisional activations. The concurrent ECD interactions between the activated protein cations and electrons resulted in extensive fragmentations (see Figure 2e). The reversed sequence of events, in which activation of noncovalent bonds took place after ECD fragmentation, also produced

equally effective fragmentations.

This 'in-beam' activation showed a good efficiency of providing 53 inter-residue bonds information. The simultaneous operation of both activation and ECD events gave a noticeable difference in between the resulting spectra. For example, in 'in-beam' ECD mass spectra, a significant amount of *b*, *y* type fragment ions are observed, which is strongly indicative of high internal-energy increases in the precursor ions. It is also noticeable that in the resulting mass spectra, *z*<sup>•</sup> ions appeared less frequently than in other AI-ECD spectra. This implies that 'in-beam' ECD condition is very harsh since *z*<sup>•</sup> ions is usually known to experience further decomposition at high temperatures.

Despite its aforementioned advantages, in-beam ECD MS has a limitation as an AI-ECD tool. The limitation is due to its operation procedure which would not permit the isolation of the protein cations of interest. However, it demonstrated a powerful protein sequencing ability, which will be very useful in characterizing a single protein species that is pre-fractionated.

### Summary and Conclusions

In the present study, various activation methods were tested in conjunction with an ECD application for the purpose of comparing their efficiencies and practical feasibilities. A multitude of different resources utilized include CO<sub>2</sub> IR laser irradiation, collisions, blackbody infrared radiation, and in-beam activation. Bovine ubiquitin 7+ cations, (M + 7H)<sup>7+</sup>, with 76 constitutive amino acids (8.6 kDa) were chosen as a model system. These cations were previously shown to provide marginal sequence information when analyzed by regular ECD with no pre-activation step. Limited 'apparent' fragmentations in ubiquitin 7- ECD experiments are due to prevailing noncovalent bonds that exist across the entire protein backbone. To gain more detailed protein sequence information, various activation methods were tested by adding sufficient internal energy to eliminate noncovalent bonds within the protein cations. A variety of activation methods showed a comparable effectiveness in enhancing the ECD fragmentation. In terms of the number of fragmented inter-residue bonds, IR laser/blackbody infrared radiation, and 'in-beam' activation were equally efficient with ~70% sequence coverage, while collisions were less productive (45 out of 75 inter-residue bonds). The collisional activation was not optimization-friendly since it had a narrow range of optimal operation conditions. In view of practical feasibility, IR laser radiation was observed to surpass the other activation tools. The IR laser operation could be controlled precisely, reproducibly, and promptly by use of a controllable beam length. Blackbody infrared radiation was excellent in various aspects, except for its long preparation time needed to raise and subsequently lower down the ICR cell temperature. As previous studies indicated, 'in-beam' activation showed an excellent effectiveness in characterizing a pre-fractionated single kind of protein species. However, its inherent

procedure did not allow for isolating the protein cations of interest during its operation, and thus set a difficult technical drawback in using this method universally as an analysis tool for protein mixtures.

**Acknowledgements.** Authors are very thankful to Kathrin Breuker, Ying Ge, and Siu Kwan Sze for their valuable discussions and the National Institutes of Health (Grant GM 16609) for generous financial support. OHB is grateful to grant R08-2003-000-10493-0 from the Korea Research Foundation.

### References

- Zubarev, R. A.; Kelleher, N. L.; McLafferty, F. W. *J. Am. Chem. Soc.* **1998**, *120*, 3265.
- Zubarev, R. A.; Horn, D. M.; Fridriksson, E. K.; Kelleher, N. L.; Kruger, N. A.; Lewis, M. A.; Carpenter, B. K.; McLafferty, F. W. *Anal. Chem.* **2000**, *72*, 563.
- Horn, D. M.; Ge, Y.; McLafferty, F. W. *Anal. Chem.* **2000**, *72*, 4778.
- Sze, S. K.; Ge, Y.; Oh, H. B.; McLafferty, F. W. *Proc. Natl. Acad. Sci. U.S.A.* **2002**, *99*, 1774.
- Sze, S. K.; Ge, Y.; Oh, H. B.; McLafferty, F. W. *Anal. Chem.* **2003**, *75*, 1599.
- Zubarev, R. A. *Mass Spectrom. Rev.* **2003**, *22*, 57.
- Cooper, H. J.; Håkansson, K.; Marshall, A. G. *Mass Spectrom. Rev.* **2005**, *24*, 201.
- Kuster, B.; Mann, M. *Curr. Opin. Chem. Biol.* **1998**, *8*, 393.
- Kelleher, N. L.; Lin, H. Y.; Valaskovic, G. A.; Aaserud, D. J.; Fridriksson, E. K.; McLafferty, F. W. *J. Am. Chem. Soc.* **1999**, *121*, 806.
- Forbes, A. J.; Mazur, M. T.; Kelleher, N. L.; Patel, H. M.; Walsh, C. T. *Proteomics* **2001**, *1*, 927.
- Zabrouskov, V.; Giacomelli, L.; van Wijk, K. J.; McLafferty, F. W. *Molecular and Cellular Proteomics* **2003**, *2*, 1253.
- Ge, Y.; Lawhorn, B. G.; Elnaggar, M.; Sze, S. K.; Begley, T. P.; McLafferty, F. W. *Protein Sci.* **2003**, *12*, 2320.
- Taylor, G. K.; Kim, Y. B.; Forbes, A. J.; Meng, F.; McCarthy, R.; Kelleher, N. L. *Anal. Chem.* **2003**, *75*, 4081.
- Kruger, N. A.; Zubarev, R. A.; Carpenter, B. K.; Kelleher, N. L.; Horn, D. M.; McLafferty, F. W. *Int. J. Mass Spectrom.* **1999**, *182/183*, 1.
- Oh, H. B.; Breuker, K.; Sze, S. K.; Ge, Y.; Carpenter, B. K.; McLafferty, F. W. *Proc. Natl. Acad. Sci. U.S.A.* **2002**, *99*, 15863.
- Breuker, K.; Oh, H. B.; Horn, D. M.; Cerda, B. A.; McLafferty, F. W. *J. Am. Chem. Soc.* **2002**, *124*, 6407.
- Marshall, A. G.; Wang, T. C. L.; Ricca, T. L. *J. Am. Chem. Soc.* **1985**, *107*, 7893.
- Gauthier, J. W.; Trautman, T. R.; Jacobson, D. B. *Anal. Chim. Acta* **1991**, *246*, 211.
- Yu, S. H.; Lee, S. Y.; Jung, G. S.; Oh, H. B. *Bull. Korean Chem. Soc.* **2004**, *25*, 1477.
- Han, S. Y.; Lee, S. Y.; Oh, H. B. *Bull. Korean Chem. Soc.* **2005**, *26*, 740.
- Horn, D. M.; Zubarev, R. A.; McLafferty, F. W. *J. Am. Soc. Mass Spectrom.* **2000**, *11*, 320.
- Valentine, S. J.; Counterman, A. E.; Clemmer, D. E. *J. Am. Soc. Mass Spectrom.* **1997**, *8*, 954.
- Li, J.; Taraszka, J. A.; Counterman, A. E.; Clemmer, D. E. *Int. J. Mass Spectrom.* **1999**, *185/186/187*, 37.
- Purves, R. W.; Barnett, D. A.; Ellis, B.; Guevremont, R. *J. Am. Soc. Mass Spectrom.* **2001**, *12*, 894.
- Myung, S.; Badman, E. R.; Lee, Y. J.; Clemmer, D. E. *J. Phys. Chem. A* **2002**, *106*, 9976.
- Senko, M. W.; Speir, J. P.; McLafferty, F. W. *Anal. Chem.* **1994**, *66*, 2801.